

# Nanoparticle-coated microcrystals†

Muthu Murugesan, Douglas Cunningham, José-Luis Martínez-Albertos, Ranko M. Vrcelj and Barry D. Moore\*

Received (in Cambridge, UK) 21st January 2005, Accepted 4th April 2005

First published as an Advance Article on the web 20th April 2005

DOI: 10.1039/b501046b

Coprecipitation provides a rapid high-yield method for self-assembly of nanoparticles on the surface of flat water-soluble crystalline surfaces and a simple immobilisation technique prior to storage or thermal and chemical modification.

Self-assembly of nano-structured architectures can be used to produce new materials with interesting optical, electronic, magnetic and catalytic properties.<sup>1</sup> A recent focus has been the conjugation of biomolecules to nanoparticles in order to direct their organisation into larger structures.<sup>2</sup> This follows on from earlier work that demonstrated that nanoparticles could be bound to pre-existing biological and synthetic structures chemically modified or patterned so as to provide a template for their attachment and organization.<sup>3,4</sup> In this paper we describe an alternative approach where the nanostructured particles are prepared directly from a solution of nanoparticles and ions or small molecules – a bottom-up self-assembly process.

As illustrated in Fig. 1 the process relies on rapid coprecipitation of two components, one of which forms crystals and one of which forms a surface coating, here the nanoparticles. A near saturated aqueous solution of the crystalline component (*e.g.* salt or amino-acid) is prepared and nanoparticles dissolved into it. This mixture is added dropwise with vigorous mixing to a large excess of water-miscible solvent in which both components are poorly soluble. The

water from the mixture immediately dissolves into the solvent, very high super-saturations are rapidly reached and the two components are forced to co-precipitate together. A key finding is that the only observable solid-state products of this process are microcrystals coated with nanoparticles – phase separation leading to a mixture of crystals and nanoparticle-aggregates does not occur. Similar results have been obtained for a range of water-soluble nanoparticles and with both ionic and molecular crystals. We have termed this generic and previously un-remarked self-organization phenomenon, crystal lattice mediated self-assembly (CLAMS).<sup>5</sup> Significantly the process is equally applicable to biomolecules and can also be used for coating peptides, proteins and nucleic acids onto microcrystals.<sup>5</sup>

The preparation of gold nanoparticle-coated potassium sulfate microcrystals provides a practical example of the process. Water soluble gold nanoparticles (AuNp) were prepared according to Murray *et al.*<sup>6</sup> by reduction of the gold salt, HAuCl<sub>4</sub> with KBH<sub>4</sub> in the presence of the short thiol terminated peptide, tiopronin (*N*-(2-mercaptopropionyl)glycine) in a 6 : 1 mixture of methanol and acetic acid. These aqueous soluble nanoparticles were purified by precipitation with methanol and exhibit an average size of  $3.1 \pm 1.0$  nm as deduced from the shoulder in the visible absorption spectra at 522 nm. In a typical experiment, AuNp ( $21 \text{ mg}\cdot\text{ml}^{-1}$ ) were dissolved in a concentrated aqueous solution of K<sub>2</sub>SO<sub>4</sub> ( $120 \text{ mg}\cdot\text{ml}^{-1}$ ) and an aliquot (300  $\mu\text{l}$ ) of this solution added dropwise to 60 ml of dry acetonitrile with rapid magnetic stirring. This results in immediate coprecipitation of the salt and AuNp. The dark precipitate may be isolated by filtration on a 0.2  $\mu\text{m}$  membrane filter or else stored in dry acetonitrile saturated with K<sub>2</sub>SO<sub>4</sub>.‡

A representative SEM image of the precipitate is shown in Fig. 2.§ It can be seen to be made up almost entirely of square or rectangular tile-like microcrystals with no discernible aggregates or else amorphous particles. The absence of any sizeable non-crystalline particles in the SEM images suggests that the nanoparticles present in the sample must be bound to the microcrystals because free nanoparticles and small aggregates of nanoparticles would pass through the 0.2 micron collection filter. In this example the precipitate is expected to contain ~15 wt% of nanoparticles but by varying the concentration of nanoparticles in the initial aqueous mixture the loading can be made higher or lower. As the loading is increased the precipitate becomes finer and darker but precipitates more rapidly because of the higher density.

Redissolution of the AuNp-coated K<sub>2</sub>SO<sub>4</sub> microcrystals into water is found to be very rapid giving a clear solution and a visible absorption spectrum identical to that obtained for the starting nanoparticles. The crystals therefore provide a convenient way of storing the nanoparticles in the solid-state without aggregation.

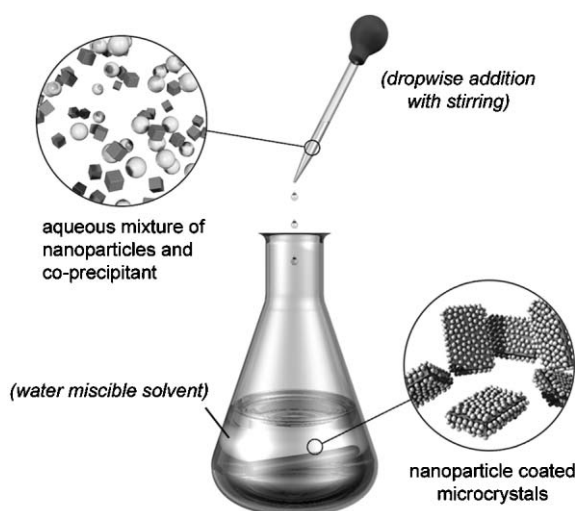
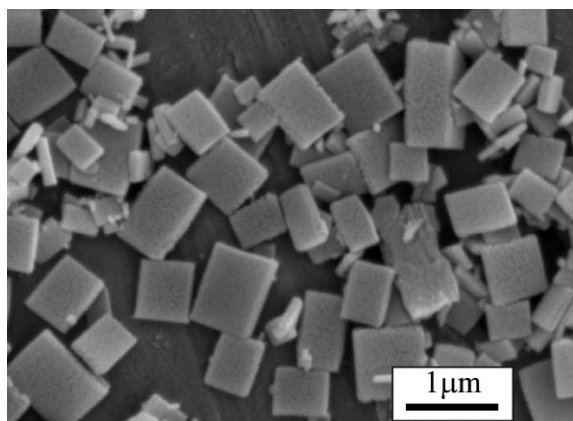


Fig. 1 Process for preparing nanoparticle-coated microcrystals.

† Electronic supplementary information (ESI) available: unit cell parameters, DSC of pure AuNp, enthalpy vs. loading plot. See <http://www.rsc.org/suppdata/cc/b5/b501046b/>

\*b.d.moore@strath.ac.uk



**Fig. 2** SEM image of AuNp-coated  $K_2SO_4$  microcrystals.

When the microcrystals were suspended in supersaturated  $K_2SO_4$  solution, the nanoparticles again rapidly dissolved, but left behind pale insoluble  $K_2SO_4$  crystals stripped of their coating. The visible absorbance at 520 nm was measured to assess the concentration of AuNp redissolved back into saturated  $K_2SO_4$  from samples prepared with different amounts of nanoparticles. As can be seen in Fig. 3 the absorbance correlated linearly with loading as expected if all the nanoparticles are located on the outer faces of the microcrystals. From geometric considerations it can be estimated that the theoretical surface coverage of nanoparticles moves from sub-monolayer (5 wt%) through monolayer (16 wt%) to multilayer (25 wt%). The quantitative binding of nanoparticles to the crystals, even at high surface coverage, is a good indication that a mechanism different from simple adsorption to pre-formed crystals is operating.

Powder X-ray diffraction studies also showed indistinguishable diffraction patterns for coated and uncoated crystals and no amorphous material, again consistent with surface coverage rather than inclusion. The unit cell parameters correspond to the arcanite structure and surface orientation effects allow the major 'tile-face' to be assigned to the (001) Miller planes<sup>†</sup>.

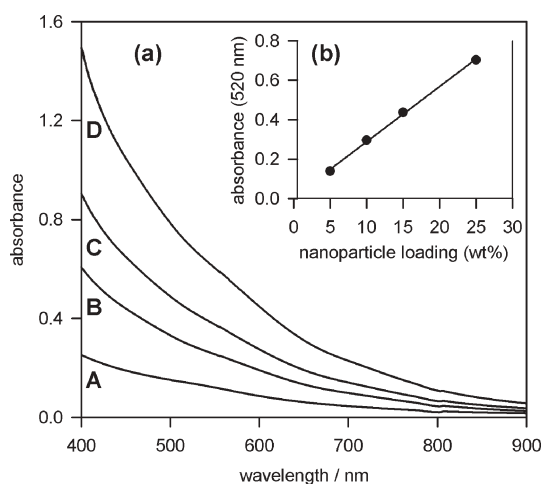


**Fig. 3** (a) UV-Visible spectra of Au-tiopronin nanoparticles removed from the microcrystal surface at different loadings: A) 5 wt%, B) 10 wt%, C) 15 wt% and D) 25 wt%. (b) Plot of absorbance at 520 nm at different nanoparticle loadings on microcrystals.

The tile-like morphology of the microcrystals which are generally less than 200 nm thick was expected to allow direct TEM imaging of the  $\sim 3$  nm nanoparticles on the microcrystal surface. In practice this proved impossible because of the extreme sensitivity of  $K_2SO_4$  crystals towards beam damage.<sup>¶</sup> This has been noted before for sulfate crystals. At low resolution the crystals exhibited high contrast in the beam and the faces appear to be smooth, consistent with the expected coherent coating of nanoparticles. However, at the higher electron beam intensity needed to resolve individual nanoparticles on the surface, the crystals were found to rapidly decompose. This process takes place albeit more slowly even at intermediate magnification as illustrated in Fig. 4. Within less than a minute exposure to the beam the microcrystals have disappeared. During this time it is sometimes possible to observe plumes of high contrast material, presumably nanoparticles, being expelled from the surface.

An alternative and sensitive way of obtaining information about the surface of colloidal particles such as the microcrystals is to measure their Zeta potential. This parameter varies according to the type and density of charged species present on the surface. Because the microcrystals are water soluble the measurements were made in acetonitrile following coprecipitation, rinsing and dilution in the same solvent.<sup>||</sup> The values obtained were as follows: pure AuNps  $-62.6 \pm 1.0$  mV, uncoated  $K_2SO_4$  microcrystals  $-17.8 \pm 6.7$  mV, AuNp-coated  $K_2SO_4$  microcrystals  $-52.3 \pm 1.2$  mV. In the case of the pure AuNp the pendant carboxyl groups of the protective tiopronin monolayer are known to be partially ionised so the negative Zeta potential for these nanoparticles is as expected. The uncoated microcrystals show a weakly negative Zeta potential suggesting that a small excess of sulfate ions are bound to the surface. In comparison the AuNp-coated microcrystals have a significantly more negative Zeta potential consistent with assembly of a layer of 'negative' nanoparticles on the crystal surfaces. The assembly of negative nanoparticles onto what is ostensibly a

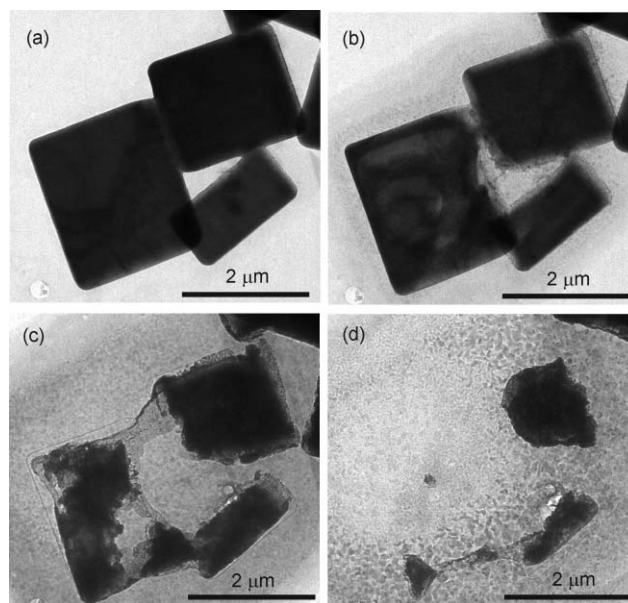


**Fig. 4** Decomposition of AuNp-coated  $K_2SO_4$  microcrystals. Images (a)–(d) taken at 5 seconds time intervals following exposure to 2 seconds. Samples have 25 wt% loading.

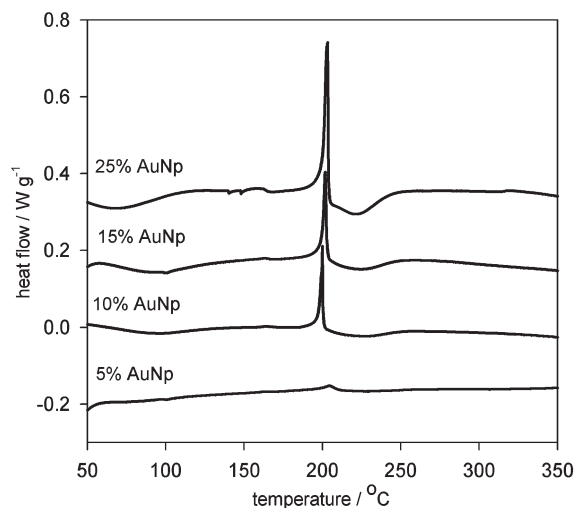


**Fig. 5** DSC traces for nanoparticle-coated microcrystals of different loadings. The samples were heated at  $10\text{ }^{\circ}\text{C min}^{-1}$ .

negative template clearly shows that the CLAMS process is not driven by a simple electrostatic binding mechanism.

$\text{K}_2\text{SO}_4$  forms a very stable crystal lattice that can be heated to  $> 550\text{ }^{\circ}\text{C}$  with no phase change or decomposition process<sup>7</sup> while 3 nm AuNp are reported to fuse around  $250\text{ }^{\circ}\text{C}$ .<sup>8</sup> It should therefore be possible to sinter together adjacent AuNp on the crystal surface. The thermograms obtained *via* differential scanning calorimetry for various loadings of nanoparticles on  $\text{K}_2\text{SO}_4$  are shown in Fig. 5\*\*. The sharp positive peak corresponds to an exotherm and the subsequent broad negative peak arises from an endotherm. The endotherm coincides with loss of ligand as shown by thermo-gravimetric measurements.<sup>6</sup> The exotherm occurs at  $200\text{ }^{\circ}\text{C}$  before any significant ligand loss and clearly increases with AuNp wt%.

A similar but much broader peak is observed with pure nanoparticle powder†. The exotherm is therefore assigned to sintering together of adjacent nanoparticles which is expected to be thermodynamically favourable once the protective tiopronin ligands become labile. At 10 wt% and above the enthalpy associated with this exotherm was observed to increase linearly with loading. However, at lower loadings the exotherm does not follow this trend and is less than the extrapolated value. For example at 5 wt% the value is around half that expected†. This is consistent with the nanoparticles being on average further apart so that sintering occurs less often.

The work described shows that AuNp-coated microcrystals can be prepared straightforwardly by a coprecipitation approach, providing a novel way of immobilising nanoparticles over a high-surface area. Other types of water soluble nanoparticles can also be used in the process including semi-conductor nanoparticles and larger metal nanoparticles (unpublished results).†† When coated onto microcrystals nanoparticles can be stored conveniently without aggregation and are amenable to further processing steps including sintering, chemical modification and inclusion into polymers. Subject to the correct solubility characteristics many nanoparticle/crystal combinations are possible and potential

applications include electronic and optical devices, coatings, sensors and catalysts.<sup>1,9</sup> Another interesting future direction under investigation is coimmobilisation and imaging of nanoparticles and biomolecules, and their conjugates on the inherently flat crystal surfaces.

This work was sponsored by the European Union (ESCHER, IST-2001-33287) under the Future Emerging Technologies proactive initiative Nanotechnology Information Devices. We thank Henk Vos for help with graphic design.

**Muthu Murugesan, Douglas Cunningham, José-Luis Martínez-Albertos, Ranko M. Vrcelj and Barry D. Moore\***

*Department of Pure & Applied Chemistry, Thomas Graham Building, University of Strathclyde, 295 Cathedral Street, Glasgow, UK G1 1XL. E-mail: b.d.moore@strath.ac.uk; Fax: +44 141 548 4822; Tel: +44 141 548 2301*

## Notes and references

‡ On storage in solvent there are no obvious changes to the size of crystals or loss of nanoparticle coating.

§ SEM measurements were made using a JEOL 6400 scanning electron microscope.

¶ TEM measurements were carried out using a ZEISS 902 transmission electron microscope. A drop of acetonitrile solution containing Au-tiopronin nanoparticle-coated  $\text{K}_2\text{SO}_4$  microcrystals was placed on a carbon coated copper grid (400 mesh) and excess solvent was removed with tissue paper. The grid was dried in air and TEM measurements were made.

|| Zeta potential measurements were made using a Malvern Instruments Zetasizer 2000 in dry acetonitrile medium.

\*\* DSC experiments were made using a TA Instruments DSC Q1000. The samples were taken in aluminium pans and measurements were carried out in nitrogen atmosphere (60 ml/min).

†† Zwitterionic crystal forming materials can be used to prevent the aggregation of large nanoparticles seen at high salt concentrations.

- 1 A. N. Shipway, E. Katz and I. Willner, *ChemPhysChem*, 2000, **1**, 18; A. Huczko, *Appl. Phys. A*, 2000, **70**, 365; H. Zeng, J. Li, J. P. Liu, Z. L. Wang and S. Sun, *Nature*, 2002, **420**, 395.
- 2 C. M. Niemeyer, *Angew. Chem., Int. Ed.*, 2001, **40**, 4128; Z. Li, S.-W. Chung, J.-M. Nam, D. S. Ginger and C. A. Mirkin, *Angew. Chem., Int. Ed.*, 2003, **42**, 2306; A. G. Kanaras, Z. Wang, A. D. Bates, R. Cosstick and M. Brust, *Angew. Chem., Int. Ed.*, 2003, **42**, 191; E. Katz and I. Willner, *Angew. Chem., Int. Ed.*, 2004, **43**, 6042.
- 3 S. L. Burkett and S. Mann, *Chem. Commun.*, 1996, **3**, 321; W. Shenton, D. Pum, U. B. Sleytr and S. Mann, *Nature*, 1997, **389**, 585; M. Li, H. Schnablegger and S. Mann, *Nature*, 1999, **402**, 393; S. R. Hall, H. Bolger and S. Mann, *Chem. Commun.*, 2003, **22**, 2784; J. L. Coffey, S. R. Bigham, X. Li, R. F. Pinizzotto, Y. G. Rho, R. M. Pirtle and I. L. Pirtle, *Appl. Phys. Lett.*, 1996, **69**, 3851; S. Behrens, K. Rahn, W. Habicht, K.-J. Böhm, H. Rösner, E. Dinjus and E. Unger, *Adv. Mater.*, 2002, **14**, 1621; R. A. McMillan, C. D. Paavola, J. Howard, S. L. Chan, N. J. Zaluzec and J. D. Trent, *Nat. Mater.*, 2002, **1**, 247.
- 4 I. W. Hamley, *Nanotechnology*, 2003, **14**, R39; D. Wang and H. Möhwald, *J. Mater. Chem.*, 2004, **14**, 459; F. Caruso, *Adv. Mater.*, 2001, **13**, 11.
- 5 M. Kreiner, B. D. Moore and M. C. Parker, *Chem. Commun.*, 2001, 1096; M. Kreiner, G. Fuglevand, B. D. Moore and M. C. Parker, *Chem. Commun.* (DOI: 10.1039/b501045d, this issue).
- 6 A. C. Templeton, S. Chen, S. M. Gross and R. W. Murray, *Langmuir*, 1999, **15**, 66.
- 7 W. P. Wueffling, F. P. Zamborini, A. C. Templeton, X. Wen, H. Yoon and R. W. Murray, *Chem. Mater.*, 2001, **13**, 87.
- 8 R. H. Chen, R.-J. Wang, T. M. Chen and C. S. Shern, *J. Phys. Chem. Solids*, 2000, **61**, 519.
- 9 A. G. Nassiopoulou, A. Zoy, V. Ioannou-Sougleridis, A. Olzierski, A. Travlos, J. L. Martínez-Albertos and B. Moore, *Nanotechnology*, 2004, **15**, 352.